On the Variational Reaction Theory for Dielectric Waveguides

RUEY-BEEI WU AND CHUN HSIUNG CHEN

Abstract — **By the reaction concept, a variational theory is established for treating the scattering and propagation problem associated with a dielectric waveguide which is illuminated by an obliquely incident plane wave. The theory is characterized by properly absorbing radiation and continuity conditions into the variational equation. This equation is then solved by the finite-element method together with the frontal solution technique. In this paper, the propagation constants of the guide are obtained by the procedure of searching for the poles of the scattering coefficients when an inhomogeneous wave is incident. Two most attractive features of this approach are the avoidance of the spurious modes and the accuracy of the results even for the modes near cutoff. Although the proposed theory may be applied to dielectric waveguides of arbitrary cross section, only the one with rectangular shape is investigated in detail. Also included in this study are numerical results for the propagation constants in discussing the effects due to differences in refractive indices, aspect ratios, and index profiles.**

I. Introduction

DIELECTRIC WAVEGUIDES find various applications in optical and millimeter-wave spectra. Hence, various methods have been proposed to examine their propagation characteristics. For homogeneous rectangular waveguides, circular-harmonic computer analysis [1] and some approximate methods [2], [3] have been adopted by some investigators. For more complex waveguides with complicated geometry and inhomogeneous material, the finite-element method [4]–[7] and the finite-difference method [8] may be applied to tackle the problem. By extending the ideas in treating a metallic waveguide, the existing literature assumes that the field outside the dielectric structure (the exterior field) vanishes at some distance from the core [4], [6], [8] or decays in a prescribed manner [5], [7]. Thus, to give accurate results, an artificial boundary at a large enough distance from the guide must be chosen in the process of solution. This is usually accompanied by the appearance of many spurious modes and a deficit in computer memory and CPU time. Besides, the results are still unsatisfactory for the modes near cutoff due to the improper assumption on the artificial boundary.

To resolve it, the radiation condition at infinity and the continuity conditions across a suitable boundary must be considered. This idea is properly absorbed in our study and Goell's work [1]. With this, a complicated set of equations are then formed and the conventional methods of solving matrix eigenvalue equations fail. The Newton's method can thus be employed to search for the propagation constants so that the determinant of the matrix vanishes [1]. However, as suggested by the work of wave propagation in a slab structure [9], [10], this study adopts an equivalent but more physical searching scheme based on the fact that the propagation constants are actually the poles of the scattering coefficients when an inhomogeneous wave is incident. The combination of the above two ideas has the advantages of avoiding the spurious modes in the matrix eigenvalue solution and providing accurate results for the modes near cutoff.

The problems of electromagnetic scattering by a dielectric cylinder have been conducted [11], [12] only for the normally incident case. The boundary conditions are of the Dirichlet type or the Neumann type depending on whether the E-wave ($H_z = 0$) or H-wave ($E_z = 0$) is considered. The corresponding variational equation is thus easy to obtain by conversion from an operator equation [12]. But it becomes difficult for the obliquely incident case since the operator is no longer self-adjoint and the boundary conditions are of the mixed type. Recently, a methodology called variational electromagnetics [13], [14] has been established to achieve the required variational equation from a fundamental variational principle. In their works, an adjoint operator which is unnecessary to solve must be found in advance.

In this paper, the reaction concept [15] is employed directly to obtain the required variational equation with the adjoint operator accompanied automatically. The new theory is easy to apply to more complicated problems, which is another feature of this approach. Since the exterior field is expanded by the radiation condition into an eigenfunction series [16] and is then coupled to the boundary field by continuity conditions, the resultant variational equation contains only the field defined within a bounded region. In this study, the equation will be solved by the finite-element method [17] coupled with the frontal solution technique [18].

As an application of the new theory, the rectangular dielectric waveguide will be examined more thoroughly, which also includes the computational results for propagation characteristics corresponding to various guide parameters.

Manuscript received July 31, 1984; revised November 8, 1984. This work was supported in part by the National Science Council, Republic of China, under Grant NSC74-0608-E002-02.

The authors are with the Department of Electrical Engineering, National Taiwan University, Taipei, Taiwan, R.O.C.

0018-9480/85/0600-0477$01.00 ©1985 IEEE

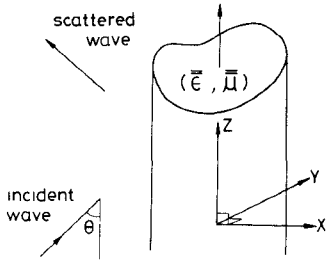

Fig. 1. Geometry of an arbitrarily shaped, inhomogeneous, and anisotropic dielectric waveguide illuminated by an obliquely incident plane wave.

II. Statement of the Problem

This study considers a uniform dielectric waveguide illuminated by a plane wave as shown in Fig. 1. The guide is arbitrary in shape and consists of material with inhomogeneity and anisotropy. The permittivity tensor $\bar{\bar{\epsilon}}$ and permeability tensor $\bar{\bar{\mu}}$ of the material are functions of x and y, but may be neither symmetric nor Hermitian. Without loss of generality, we assume that a plane wave is obliquely incident on the waveguide at an angle θ with respect to the z-axis. The field quantities then must have the same phase factor $e^{j(\omega t-\beta z)}$, where β is the wavenumber in the z-direction and is related to the wavenumber k_0 in free space by

$$\beta = k_0 \cos\theta. \tag{1}$$

For excitation by a source or by incident waves other than a plane wave, the field in free space can be expressed, by a Fourier integral, as the superposition of plane waves with the wavenumber in the z-direction in the range $|\beta| < \infty$. Hence, in addition to the waves with propagation directions in the angular range $0 \leqslant \theta \leqslant \pi$, i.e., $|\beta| \leqslant k_0$, there are waves with $|\beta|$ greater than k_0. Waves of this type, which may be guided by the waveguide, are known as inhomogeneous waves [19] and will be emphasized in this paper.

To facilitate the analysis, we shall write the tensors as

$$\bar{\bar{\epsilon}} = \begin{bmatrix} \epsilon_{xx} & \epsilon_{xy} & \epsilon_{xz} \\ \epsilon_{yx} & \epsilon_{yy} & \epsilon_{yz} \\ \epsilon_{zx} & \epsilon_{zy} & \epsilon_{zz} \end{bmatrix} = \begin{bmatrix} \bar{\bar{\epsilon}}_{tt} & \bar{\epsilon}_{tz} \\ \bar{\epsilon}_{zt}^T & \epsilon_{zz} \end{bmatrix}$$

$$\bar{\bar{\mu}} = \begin{bmatrix} \mu_{xx} & \mu_{xy} & \mu_{xz} \\ \mu_{yx} & \mu_{yy} & \mu_{yz} \\ \mu_{zx} & \mu_{zy} & \mu_{zz} \end{bmatrix} = \begin{bmatrix} \bar{\bar{\mu}}_{tt} & \bar{\mu}_{tz} \\ \bar{\mu}_{zt}^T & \mu_{zz} \end{bmatrix}. \tag{2}$$

Here, the subscript t means the component transverse to the z-direction, and the superscript T means the transpose of a matrix. In what follows, we shall use the decomposition for vectors and the del operator:

$$\bar{A} = A_x\hat{x} + A_y\hat{y} + A_z\hat{z} = \bar{A}_t + A_z\hat{z}$$

$$\nabla = \frac{\partial}{\partial x}\hat{x} + \frac{\partial}{\partial y}\hat{y} + \frac{\partial}{\partial z}\hat{z} = \nabla_t - j\beta\hat{z}. \tag{3}$$

The time and space harmonic dependence $e^{j(\omega t-\beta z)}$ is assumed and omitted throughout this paper.

III. Variational Formulation

Let us establish a variational formulation for the two-dimensional scattering problem defined by Fig. 1. In other words, we try to find a functional I of a "trial field" such that its first variation δI vanishes at the true field of the solution system [13], [14]. For this, we consider a trial field $(\bar{E}, \bar{H})$ supported by the trial sources

$$\bar{J} = \nabla \times \bar{H} - j\omega\bar{\bar{\epsilon}}\cdot\bar{E}$$
$$\bar{M} = -\nabla \times \bar{E} - j\omega\bar{\bar{\mu}}\cdot\bar{H}. \tag{4}$$

Note that these sources are zero in the solution system. Thus, the reaction [15] between any arbitrary test field $(\delta\bar{E}^a, \delta\bar{H}^a)$ and the trial sources $(\bar{J}, \bar{M})$ should vanish when the trial field is equal to the true field, i.e.,

$$\delta I = \int (\delta\bar{E}^a\cdot\bar{J} - \delta\bar{H}^a\cdot\bar{M})\, d\Omega = 0 \tag{5}$$

where the integration extends over the whole space. Note also that the test field $(\bar{E}^a, \bar{H}^a)$ may be identified with the adjoint field of the previous study [13], [14].

Equation (5) is general but difficult of access unless we can add some constraints to the trial sources. One suitable simplification is to choose the (E_z, H_z) formulation, which is equivalent to the constraint $\bar{J}_t = 0$ and $\bar{M}_t = 0$. Together with (4), the transverse components of the trial field $(\bar{E}_t, \bar{H}_t)$ can thus be related to the longitudinal ones (E_z, H_z) by

$$\begin{bmatrix} \bar{E}_t \\ \bar{H}_t \end{bmatrix} = \begin{bmatrix} j\omega\bar{\bar{\epsilon}}_{tt} & j\beta\hat{z}\times \\ j\beta\hat{z}\times & -j\omega\bar{\bar{\mu}}_{tt} \end{bmatrix}^{-1} \cdot \begin{bmatrix} -j\omega\bar{\epsilon}_{tz} & 0 & -1 & 0 \\ 0 & j\omega\bar{\mu}_{tz} & 0 & -1 \end{bmatrix} \cdot \begin{bmatrix} E_z \\ H_z \\ \hat{z}\times\nabla_t H_z \\ \hat{z}\times\nabla_t E_z \end{bmatrix}. \tag{6}$$

Another constraint on the trial sources (J_z, M_z) is to confine them within a finite region Ω. To this end, a mathematical circle Γ of radius r_0 is chosen so that all inhomogeneous and anisotropic materials are enclosed within the circular region Ω (Fig. 2). The boundary conditions are then matched on the artificial boundary Γ instead of on the actual waveguide boundary Γ'. Since the material in region Ω_0 $(r \geqslant r_0)$ is homogeneous, we can enforce $J_z = 0$, $M_z = 0$ by expanding the trial field as the superposition of cylindrical wave functions. The field in region Ω_0 is the sum of the incident field and the scattered field, that is,

$$\begin{bmatrix} \bar{E} \\ \bar{H} \end{bmatrix} = \begin{bmatrix} \bar{E}^i \\ \bar{H}^i \end{bmatrix} + \begin{bmatrix} \bar{E}^s \\ \bar{H}^s \end{bmatrix} \tag{7}$$

where the superscripts i and s denote the incident and scattered parts, respectively. The longitudinal components of the incident field and the scattered field can be expressed as

$$\begin{bmatrix} E_z^i \\ \eta_0 H_z^i \end{bmatrix} = \sum_m \begin{bmatrix} e_m^i \\ h_m^i \end{bmatrix} J_m(k_t r)\cdot e^{jm\phi}$$

$$\begin{bmatrix} E_z^s \\ \eta_0 H_z^s \end{bmatrix} = \sum_m \begin{bmatrix} e_m^s \\ h_m^s \end{bmatrix} H_m^{(2)}(k_t r)\cdot e^{jm\phi} \tag{8}$$

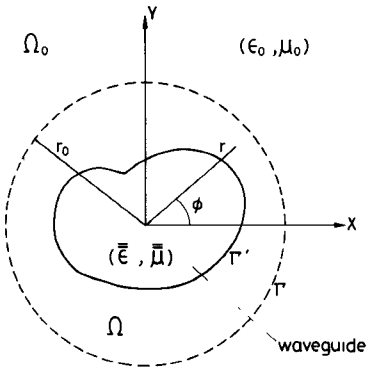

Fig. 2. Region Ω with artificial boundary Γ (a mathematical circle of radius r_0) to enclose material inhomogeneity and anisotropy. Γ' is the actual waveguide boundary.

where $k_t = \sqrt{k_0^2 - \beta^2}$ and $\eta_0 = \sqrt{\mu_0/\epsilon_0}$. The expansion coefficients for the E- and H-waves, $e_m^{i,s}$ and $h_m^{i,s}$, are related to the field on the artificial boundary by

$$\begin{bmatrix} e_m^i \\ h_m^i \end{bmatrix} = \frac{1}{2\pi}\int_0^{2\pi} \begin{bmatrix} E_z^i(r_0,\phi) \\ \eta_0 H_z^i(r_0,\phi) \end{bmatrix} \frac{e^{-jm\phi}}{J_m(k_t r_0)}\, d\phi$$

$$\begin{bmatrix} e_m^s \\ h_m^s \end{bmatrix} = \frac{1}{2\pi}\int_0^{2\pi} \begin{bmatrix} E_z^s(r_0,\phi) \\ \eta_0 H_z^s(r_0,\phi) \end{bmatrix} \frac{e^{-jm\phi}}{H_m^{(2)}(k_t r_0)}\, d\phi. \quad (9)$$

With the above constraints, the integration in (5) now extends only over the region Ω ($r \leqslant r_0$); meanwhile, the quantities involved are the longitudinal components $(\delta E_z^a, \delta H_z^a)$ and (J_z, M_z). By using (4) for (J_z, M_z), applying integration by parts, and then using (6)–(9) for the transverse components $(\bar{E}_t, \bar{H}_t)$, we finally obtain the desired variational equation

$$\delta I = 0$$

$$I = \int_\Omega d\Omega \begin{bmatrix} E_z^a \\ H_z^a \\ \hat{z}\times\nabla_t H_z^a \\ \hat{z}\times\nabla_t E_z^a \end{bmatrix}^T \cdot \begin{bmatrix} -j\omega\bar{\epsilon}_{zt}^T & 0 \\ 0 & j\omega\bar{\mu}_{zt}^T \\ -1 & 0 \\ 0 & -1 \end{bmatrix}$$

$$\cdot \begin{bmatrix} j\omega\bar{\bar{\epsilon}}_{tt} & j\beta\hat{z}\times \\ j\beta\hat{z}\times & -j\omega\bar{\bar{\mu}}_{tt} \end{bmatrix}^{-1} \cdot \begin{bmatrix} -j\omega\bar{\epsilon}_{tz} & 0 & -1 & 0 \\ 0 & j\omega\bar{\mu}_{tz} & 0 & -1 \end{bmatrix}$$

$$\cdot \begin{bmatrix} E_z \\ H_z \\ \hat{z}\times\nabla_t H_z \\ \hat{z}\times\nabla_t E_z \end{bmatrix} - \int_\Omega d\Omega \begin{bmatrix} E_z^a \\ H_z^a \end{bmatrix}^T \cdot \begin{bmatrix} j\omega\epsilon_{zz} & 0 \\ 0 & -j\omega\mu_{zz} \end{bmatrix} \cdot \begin{bmatrix} E_z \\ H_z \end{bmatrix}$$

$$- \frac{1}{2\pi k_t^2}\sum_m \int_0^{2\pi} \begin{bmatrix} E_z^a(r_0,\phi) \\ H_z^a(r_0,\phi) \end{bmatrix}^T e^{jm\phi}\, d\phi$$

$$\cdot \left\{ \begin{bmatrix} j\omega\epsilon_0 Z_m^{(2)} & -m\beta \\ -m\beta & -j\omega\mu_0 Z_m^{(2)} \end{bmatrix} \cdot \int_0^{2\pi} \begin{bmatrix} E_z(r_0,\phi) \\ H_z(r_0,\phi) \end{bmatrix} e^{-jm\phi}\, d\phi \right.$$

$$+ \left(Z_m^{(1)} - Z_m^{(2)}\right) \cdot \begin{bmatrix} j\omega\epsilon_0 & 0 \\ 0 & -j\omega\mu_0 \end{bmatrix}$$

$$\left. \cdot \int_0^{2\pi} \begin{bmatrix} E_z^i(r_0,\phi) \\ H_z^i(r_0,\phi) \end{bmatrix} e^{-jm\phi}\, d\phi \right\} \quad (10)$$

where

$$Z_m^{(1)} = k_t r_0 \cdot J_m'(k_t r_0)/J_m(k_t r_0)$$

$$Z_m^{(2)} = k_t r_0 \cdot H_m^{(2)\prime}(k_t r_0)/H_m^{(2)}(k_t r_0).$$

For the case with an inhomogeneous wave incident, we put $k_t r = -jv = -j\sqrt{\beta^2 - k_0^2}\cdot r$, which is pure imaginary. Then, the Bessel functions in (8)–(10) should be replaced by the modified Bessel functions, that is,

$$H_m^{(2)}(-jv) = \frac{2}{\pi}\cdot(j)^{m+1}\cdot K_m(v)$$

$$J_m(-jv) = (-j)^m \cdot I_m(v). \quad (11)$$

IV. Finite-Element Method with Frontal Solution Technique

The derived variational equation (10) will be solved by the finite-element method. First, the region Ω is divided into N triangular elements with N_r intervals in the radial direction and N_c intervals in the azimuthal direction. Fig. 3 shows one possible mesh division in which $N_r = 5$, $N_c = 6$, and $N = (2N_r - 1)\cdot N_c = 54$. In each element, the quadratic interpolation model and the six-node basis functions [17] are adopted in solution. The field ψ, which denotes E_z or H_z, can thus be written as

$$\psi(x,y) = \sum_{i=1}^{6} \psi_i^{(e)} B_i(l_1, l_2, l_3) \quad (12)$$

where $\psi_i^{(e)}$ is the field value (the unknown) at the node P_i of the element (Fig. 4). In this study, the six basis functions are chosen as follows.

For corner nodes

$$B_1(l_1, l_2, l_3) = l_1\cdot(2l_1 - 1), \text{ etc.}$$

For mid-side nodes

$$B_4(l_1, l_2, l_3) = 4l_1\cdot l_2, \text{ etc.} \quad (13)$$

Here, l_1, l_2, l_3 are the local coordinates in an element [17]. The transformation between original coordinates and local coordinates is defined by

$$\begin{bmatrix} x \\ y \end{bmatrix} = \sum_{i=1}^{6} \begin{bmatrix} x_i^{(e)} \\ y_i^{(e)} \end{bmatrix} B_i(l_1, l_2, l_3). \quad (14)$$

Then, we need to calculate the integrals contributed from each element. Here, analytic integration formulas are unavailable whenever the material in an element is not homogeneous; thus, numerical integration, e.g., the seven-point Gauss–Hammer quadrature formula [17], is necessary. When the incident wave is an inhomogeneous one, there may exist a curve over which the matrix in (10) is singular. Though this singularity is integrable, attention should be paid in the numerical integration. In this paper, the element boundary is chosen to be coincident with the singular curve, if any. Then the integrand is finite inside an element, and hence the quadrature formula can be employed directly.

Worthy next of separate consideration is the contribution from the boundary element, the $N+1$th element,

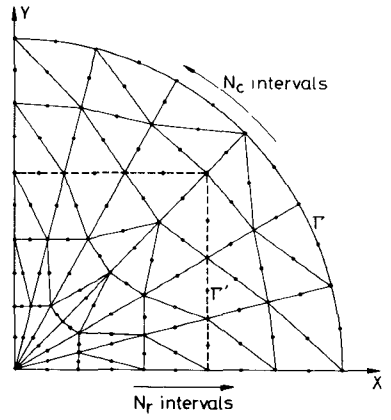

Fig. 3. Typical mesh division for rectangular dielectric waveguide. The dashed line represents the actual waveguide boundary.

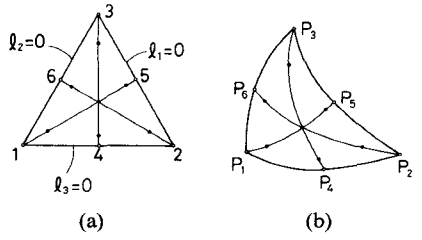

Fig. 4. Mapping of elements: (a) local coordinates, and (b) original coordinates. The circles are nodal points, while the dots are sampling points in the Gauss–Hammer quadrature formula.

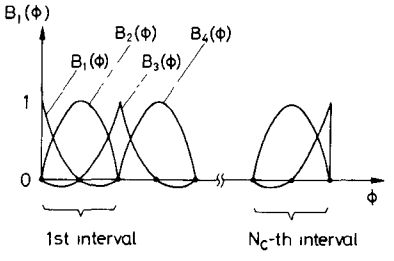

Fig. 5. Nodes on the boundary element and corresponding basis functions.

along the mathematical circle Γ. As shown in Fig. 3, the circle has been uniformly divided into N_c intervals. The field on the boundary Γ is again expressed as

$$\psi(\phi)=\sum_i \psi_i^{(N+1)} B_i(\phi) \tag{15}$$

where $\psi_i^{(N+1)}$'s are the unknown field values on Γ and $B_i(\phi)$'s are the corresponding basis functions (Fig. 5). For continuity of the fields with (12), the basis functions $B_i(\phi)$'s are also chosen as quadratic functions of ϕ in each interval. Hence, some analytic integration formulas for $\int B_i(\phi)e^{jm\phi}d\phi$ and $\int B_i(\phi)e^{-jm\phi}d\phi$ should be employed to compute the boundary-element matrix corresponding to the last term in (10).

To assure that the space harmonics in (8) can express the boundary fields at the sampled nodes properly, the number of terms included in (10) should be chosen no less than the number of nodes along the boundary. For the case shown in Fig. 3, where electric and magnetic conductors may be placed in the $x-z$ and $y-z$ planes, odd space harmonics of $2N_c+1$ terms, at least, are needed to give satisfactory results in computation.

Finally, the variational equation (10) is solved by the Ritz method. This then leads to a matrix equation

$$[P]\cdot[\Psi]=[S] \tag{16}$$

where $[\Psi]$ is the column vector composed of the nodal unknowns, while $[P]$ and $[S]$ are known matrices. The matrix $[P]$ is of the banded type and is obtained by assembling the contribution from each element. Though (16) can be solved efficiently by various numerical techniques [17], computer core memory may still be inadequate to store all the nonzero terms of $[P]$ when the system is extremely large. In such a case, the frontal solution technique [18], which is advantageous in the use of core memory, is recommended in numerical computation.

The basic ideas of this technique can be briefly described. While assembling the element matrices, the nodal unknown is eliminated as long as every element containing the node has been accounted for. The corresponding rows of $[P]$ and $[S]$, after eliminating this unknown, are stored in an auxiliary storage and are free from the core memory for the element to be assembled next. After all elements are assembled and all unknowns are eliminated, the equations in the auxiliary storage are read in reverse order and the unknowns are solved by successive back-substitution. It is the back-substitution process that takes much CPU time.

The efficiency of this technique relies on the element numbering scheme rather than the node numbering scheme. For scattering problems, the scattered field, which we are more interested in, is directly related to the boundary field. Hence, by assembling the last element corresponding to the boundary one, we may obtain a set of equations involving only the unknowns on the boundary Γ. Since the boundary field can be solved by these equations, it is unnecessary to call for the auxiliary storage to execute the time-consuming back-substitution process. For the typical mesh shown in Fig. 3, the number of total unknowns is 250 and the front-width is 36; however, the actually required core memory for handling $[P]$ is only about 650 ($\approx 36^2/2$)!

V. Numerical Results

A Fortran program for an arbitrarily shaped, inhomogeneous, and anisotropic dielectric waveguide (Fig. 1) has been implemented on a VAX-11/780 mini-computer. However, only the computational results for the guide with rectangular cross section and inhomogeneous material are presented in this paper. Especially for the rectangular one, we have made full use of the waveguide symmetries so that the computational loads may further be reduced.

The rectangular dielectric waveguide under consideration has dimension $a\times b$ $(a\geq b)$ as shown in Fig. 6(a). This study deals mainly with two specific types of refractive index, namely the step-index profile

$$n^2(x,y)=\epsilon_r(x,y)=\begin{cases} n_c^2, & |x|<a/2,\ |y|<b/2 \\ 1, & \text{elsewhere} \end{cases} \tag{17}$$

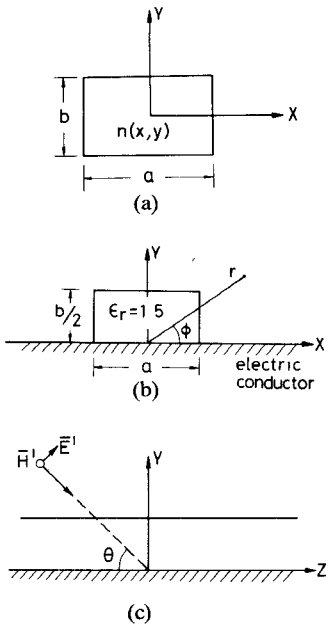

Fig. 6. Geometry of (a) rectangular dielectric guide and (b) image guide. (c) Figure to define incident E-wave and incident angle θ.

and the α-power profile

$$n^2(x,y) = n_c^2 - (n_c^2 - 1)\cdot[f(x,y)]^{\alpha} \tag{18}$$

where

$$f(x,y) = \begin{cases} \max(|2x/a|, |2y/b|), & |x| < a/2, |y| < b/2, \\ 1, & \text{elsewhere.} \end{cases}$$

Note that the α-power profile reduces to the step-index one as α tends to infinity.

First consider the image guide shown in Fig. 6(b), which is a special case of the rectangular dielectric waveguide (Fig. 6(a)) possessing the symmetry when a perfect electric conductor is inserted in the center $x-z$ plane. Let an E-wave with a propagation vector in the $y-z$ plane be incident upon the image guide with an angle θ with respect to the z-axis (Fig. 6(c)). The guide dimension is $a = \lambda_0$ and $b/2 = \lambda_0/2$, where λ_0 is the wavelength in free space. As a check of the program, we consider a step-index waveguide with dielectric constant $\epsilon_r = 1.5$. The longitudinal component of the incident field now takes the form

$$E_z^i = 2j\cdot\sin(k_0 y\cdot\sin\theta) \tag{19}$$

due to the presence of the electric conductor.

The scattering coefficients e_m^s and h_m^s, defined in (8) and (9), for various incident angles θ are shown in Fig. 7. Since the incident wave is also symmetric with respect to the $y-z$ plane, the scattering coefficients for even m vanish. For the normal incident case, i.e., $\theta = 90°$, the E- and the H-waves are separable and, hence, h_m^s's are zero. And for the oblique incident case where $\theta \neq 90°$, both E- and H-waves are excited and coupled as reflected in Fig. 7. Especially for the grazing incident case ($\theta \approx 0°$), both

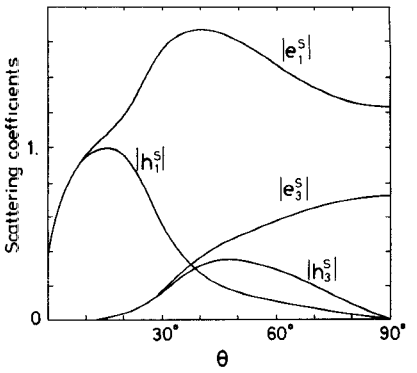

Fig. 7. Amplitude of scattering coefficients versus incident angles θ for step-index image guide. Parameters used are $a = \lambda_0$, $b/2 = \lambda_0/2$, and $\epsilon_r = n_c^2 = 1.5$.

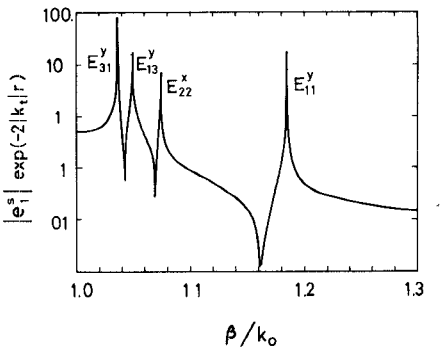

Fig. 8. Scattering coefficients for an inhomogeneous wave incident ($|\beta| > k_0$). The step-index image guide considered has parameters: $a = 2\lambda_0$, $b/2 = \lambda_0$, and $\epsilon_r = 1.5$. Depicted in the figure are four poles which correspond to guided modes E_{11}^y, E_{22}^x, E_{13}^y, and E_{31}^y.

waves are so strongly coupled that the scattered wave is dominantly an HE-wave [20].

The scattering coefficients for $|\beta| > k_0$, which can provide a significant physical implication (such as revealing the guidance of waves), are discussed in the following. Fig. 8 shows the normalized scattering coefficient $|e_1^s|\cdot\exp(-2|k_t|r)$ for the image guide as defined by Fig. 6(b). The most attractive point about the figure is that there exist poles of the scattering coefficient, which correspond to the propagation constants of guided modes in the waveguide.

Now, one may suggest two properties to facilitate the searching scheme for each pole β_0: 1) the sign of the scattering coefficient changes when β is across β_0, and 2) the reciprocal of the scattering coefficient is essentially linear near β_0. For the guide consisting of lossy material, the pole β_0 is complex. One must seek the pole in the complex plane, and the Bessel functions with complex arguments should be required. However, when the material is of low-loss tangent, the pole is near the real axis. Therefore, one need only search for two β's near the pole along the real axis and then employ the rule of "false position" to calculate the approximate β_0 [21].

The aforementioned pole searching scheme will be utilized to calculate the propagation constants of the waveguide. The corresponding dispersion curves will be given in terms of the normalized propagation constants $\mathscr{P}^2$ and the

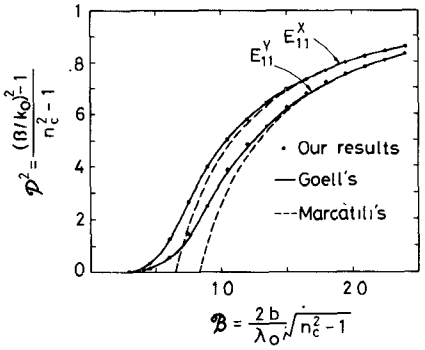

Fig. 9. Comparison of our numerical results, dispersion relations of principal modes E_{11}^x and E_{11}^y, with those of previous works. Step-index rectangular dielectric waveguide is adopted with parameters: $n_c=1.5$ and $a/b=2$.

normalized frequency $\mathscr{B}$ [1] where

$$\mathscr{P}^2=\frac{(\beta/k_0)^2-1}{n_c^2-1}$$

$$\mathscr{B}=\frac{2b}{\lambda_0}\cdot\sqrt{n_c^2-1}\,. \tag{20}$$

A note on the steps in seeking a pole is also worth mentioning. For any given $\mathscr{B}$, two points of $\mathscr{P}^2$ in the interval (0,1) are first chosen so that the scattering coefficients have a 180° phase shift. The poles can thus be found by employing the Mueller's iteration scheme of successive bisection and inverse parabolic interpolation [22]. Generally speaking, one takes six iterative steps, at most, to give satisfactory results for each pole.

Remaining is the study of the rectangular dielectric guides as shown in Fig. 6(a). Here, various symmetries with respect to the $x-z$ plane and the $y-z$ plane are utilized to reduce the computer memory and time. For instance, to discuss the principal mode E_{11}^x, which has the transverse E-field polarized dominantly in the x-direction, an electric conductor and a magnetic conductor may be placed over the $y-z$ plane and the $x-z$ plane, respectively, without disturbing the field distribution. The other principal mode E_{11}^y can be found with the two symmetries interchanged. For the step-index waveguide with aspect ratio $a/b=2$ and refractive index $n_c=1.5$, the computed dispersion relations of these two principal modes are shown as dot points in Fig. 9. They are also compared with those of Goell's [1] and Marcatili's [2] works. The excellent agreement with Goell's results, at least, supports the correctness of our program. For the typical mesh division in Fig. 3, the CPU time required on the VAX-11/780 mini-computer to compute an eigenvalue is about 2 min. It is also found that this time increases nearly proportional to the square of the total number of elements.

In Fig. 10, we examine the effect of various α-power profiles on the principal mode E_{11}^x of the rectangular waveguides with $n_c=1.5$ and $a/b=1$. Since the two principal modes are degenerate in this case, no specification on polarization is indicated. Note that for larger values of α,

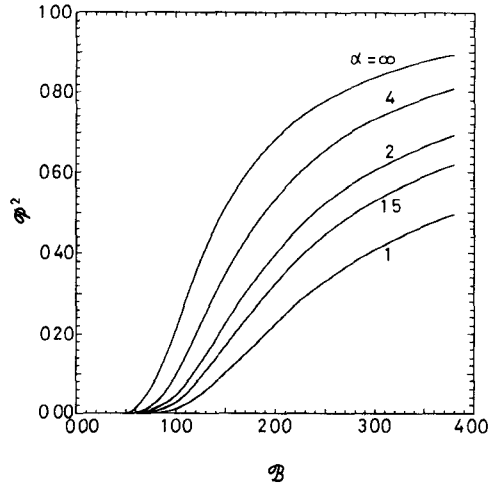

Fig. 10. Dispersion relations of principal mode E_{11}^x with α as parameters. Rectangular guide of α-power profile is considered with $a/b=1$ and $n_c=1.5$.

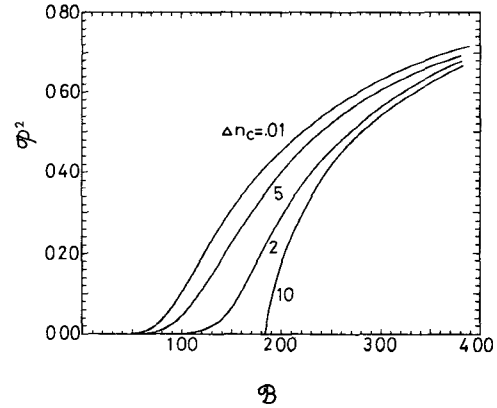

Fig. 11. Dispersion relations of principal mode E_{11}^x with $\Delta n_c\ (=n_c-1)$ as parameters. Rectangular guide of α-power profile is adopted with $a/b=1$ and $\alpha=2$.

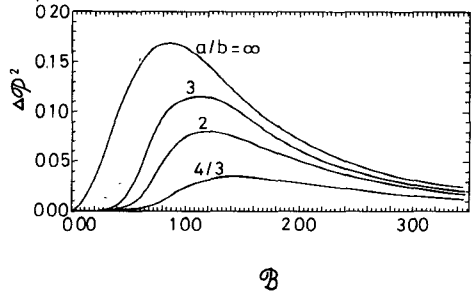

Fig. 12. Effect of aspect ratios on the difference of normalized propagation constants between two principal modes. The curves are for rectangular dielectric waveguides of α-power profile with $n_c=1.5$ and $\alpha=2$.

the corresponding propagation constant is larger, and hence the field is more confined in the guide.

The effect due to the difference in refractive indices, i.e., $\Delta n_c=n_c-1$, is presented in Fig. 11. The guides concerned here are of unity aspect ratio and parabolic index profile, i.e., $\alpha=2$.

For the waveguides with aspect ratio greater than 1.0, the two principal modes E_{11}^x and E_{11}^y are no more degenerate. The associated birefringence is important in polariza-

tion-sensitive devices. For this usage, a single-mode waveguide should be chosen based on practical consideration. In this case, the theory proposed in this paper is very promising since the fields of the two principal modes are not well confined in the waveguide structure. As an example, we consider the rectangular waveguides with a parabolic index profile and $n_c = 1.5$. The difference of the propagation constants $\Delta\beta^2$ between these two polarizations is shown in Fig. 12. Guides with various aspect ratios such as $a/b = 4/3$, 2, 3, and infinity have been considered. Note that the curve for the infinity aspect ratio is obtained from the analysis of the slab case.

VI. Conclusions

By the reaction concept, and coupled with the radiation and continuity conditions, a variational reaction theory has been established and applied to attack the problems of electromagnetic scattering by dielectric waveguides. The derived variational equation has been solved by the finite-element method together with the frontal solution technique. It has been found that more accurate results can be obtained due to the proper handling of the boundary conditions. The versatility of the new approach is reflected in the use of the finite-element method, which can easily and systematically tackle the waveguides with complex geometries and general material media. The developed program has been found very powerful due to a large reduction in core memories via the frontal solution technique so that CPU time is the only factor of limitation.

In this paper, the poles of the scattering coefficients have been investigated thoroughly and related to the propagation constants of the waveguides. The scattering analysis may also be applied to characterize the phenomena such as the longitudinal shift and the wave shaping of an incident beam. Besides, this theory can be applied easily to other complex problems. Some related works (for instance, the study of dielectric waveguide junctions or discontinuities) are in progress and will be reported in the near future.

References

[1] J. E. Goell, "A circular-harmonic computer analysis of rectangular dielectric waveguides," *Bell Syst. Tech. J.*, vol. 48, pp. 2133–2160, Sept. 1969.

[2] E. A. J. Marcatili, "Dielectric rectangular waveguide and directional coupler for integrated optics," *Bell Syst. Tech. J.*, vol. 48, pp. 2071–2102, Sept. 1969.

[3] S. Akiba and H. A. Haus, "Variational analysis of optical waveguides with rectangular cross section," *Appl. Opt.*, vol. 21, pp. 804–808, Mar. 1982.

[4] C. Yeh, S. B. Dong, and W. Oliver, "Arbitrarily shaped inhomogeneous optical fiber or integrated optical waveguides," *J. Appl. Phys.*, vol. 46, pp. 2125–2129, May 1975.

[5] C. Yeh, K. Ha, S. B. Dong, and W. P. Brown, "Single-mode optical waveguides," *Appl. Opt.*, vol. 18, pp. 1490–1504, May 1979.

[6] N. Mabaya, P. E. Lagasse, and P. Vandenbulcke, "Finite-element analysis of optical waveguides," *IEEE Trans. Microwave Theory Tech.*, vol. MTT-29, pp. 600–605, June 1981.

[7] B. M. A. Rahman and J. B. Davies, "Finite-element analysis of optical and microwave waveguide problems," *IEEE Trans. Microwave Theory Tech.*, vol. MTT-32, pp. 20–28, Jan. 1984.

[8] E. Schweig and W. B. Bridges, "Computer analysis of dielectric waveguides: A finite-difference method," *IEEE Trans. Microwave Theory Tech.*, vol. MTT-32, pp. 531–541, May 1984.

[9] R. E. Collin, *Field Theory of Guided Waves*. New York: McGraw-Hill, 1960.

[10] C. C. Su and C. H. Chen, "A fast algorithm for inhomogeneous slab scattering problem from integral equation approach," *J. Appl. Phys.*, vol. 53, pp. 6009–6014, Sept. 1982.

[11] J. H. Richmond, "Scattering by a dielectric cylinder of arbitrary cross section shape," *IEEE Trans. Antennas Propagat.*, vol. AP-13, pp. 334–341, May 1965.

[12] S. K. Chang and K. K. Mei, "Application of unimoment method to electromagnetic scattering of dielectric cylinders," *IEEE Trans. Antennas Propagat.*, vol. AP-24, pp. 35–42, Jan. 1976.

[13] S. K. Jeng and C. H. Chen, "Variational finite element solution of electromagnetic wave propagation in a one-dimensional inhomogeneous anisotropic medium," *J. Appl. Phys.*, vol. 55, pp. 630–636, Feb. 1984.

[14] S. K. Jeng and C. H. Chen, "On variational electromagnetics: Theory and applications," *IEEE Trans. Antennas Propagat.*, vol. AP-32, pp. 902–907, Sept. 1984.

[15] V. H. Rumsey, "Reaction concept in electromagnetic theory," *Phys. Rev.*, vol. 94, pp. 1483–1491, June 1954.

[16] R. F. Harrington, *Time-Harmonic Electromagnetic Fields*. New York: McGraw-Hill, 1961.

[17] O. C. Zienkiewicz, *The Finite Element Method*. New York: McGraw-Hill, 1977.

[18] E. Hinton and D. R. J. Owen, *Finite Element Programming*. New York: Academic Press, 1977.

[19] L. M. Brekhovskieh, *Waves in Layered Media*. New York: Academic Press, 1960.

[20] CSELT, *Optical Fiber Communication*. New York: McGraw-Hill, 1981.

[21] J. Todd, *Survey of Numerical Analysis*. New York: McGraw-Hill, 1962.

[22] C. F. Gerald, *Applied Numerical Analysis*. New York: Addison-Wesley, 1969.

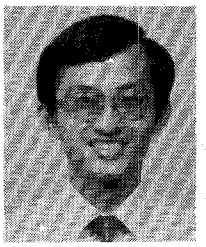

Ruey-Beei Wu was born in Tainan, Taiwan, Republic of China, on October 27, 1957. He received the B.S.E.E. degree from National Taiwan University, Taipei, Taiwan, in 1979. Since 1981, he has been studying toward the Ph.D. degree at the same university.

In 1982, he joined the faculty of the Department of Electrical Engineering, National Taiwan University, where he is now an Instructor. He is currently engaged in the area of numerical methods to electromagnetic-field problems.

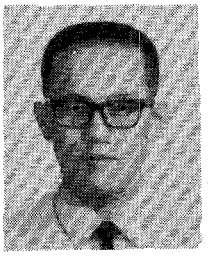

Chun Hsiung Chen was born in Taipei, Taiwan, Republic of China, on March 7, 1937. He received the B.S.E.E. degree from National Taiwan University, Taipei, Taiwan, in 1960, the M.S.E.E. degree from National Chiao Tung University, Hsinchu, Taiwan, in 1962, and the Ph.D. degree in electrical engineering from National Taiwan University in 1972.

In 1963, he joined the faculty of the Department of Electrical Engineering, National Taiwan University, where he is now a Professor. From August 1982, he has also been the Chairman of the same department. In 1974, he was a Visiting Researcher for one year at the Department of Electrical Engineering and Computer Sciences, University of California, Berkeley. His areas of interest include antenna and waveguide analysis, propagation and scattering of waves, and numerical techniques in electromagnetics.